Journal of Instrumentation

CMS Pixel Detector design for HL-LHC

To cite this article: E. Migliore 2016 *JINST* **11** C12061

Jinst

Published by IOP Publishing for Sissa Medialab

Received: *October 4, 2016*
Accepted: *December 12, 2016*
Published: *December 21, 2016*

Pixel 2016 International Workshop
September 5 – September 9, 2016
Sestri Levante, Genova, Italy

CMS Pixel Detector design for HL-LHC

E. Migliore on behalf of the CMS collaboration

Università di Torino and INFN Sezione di Torino,
via P.Giuria 1, 10125 Torino Italy

E-mail: ernesto.migliore@unito.it

Abstract: The LHC machine is planning an upgrade program which will smoothly bring the luminosity to about $7.5 \times 10^{34}\text{cm}^{-2}\text{s}^{-1}$ in 2028, to possibly reach an integrated luminosity of 3000 fb^{-1} by the end of 2037. This High Luminosity scenario, HL-LHC, will present new challenges in higher data rates and increased radiation. In order to maintain its physics reach the CMS collaboration has undertaken a preparation program of the detector known as Phase-2 upgrade. The CMS Phase-2 Pixel upgrade will require a high bandwidth readout system and high radiation tolerance for sensors and on-detector ASICs. Several technologies for the upgrade sensors are being studied. Serial powering schemes are under consideration to accommodate significant constraints on the system. These prospective designs, as well as new layout geometries that include very forward pixel discs, will be presented together with performance estimation.

Keywords: Particle tracking detectors (Solid-state detectors); Radiation-hard detectors

2016 JINST 11 C12061

doi:10.1088/1748-0221/11/12/C12061

Contents

1 Motivations and requirements

The goal of the LHC high-luminosity program (HL-LHC) is to collect an integrated luminosity of $\mathcal{L}_{\text{int}} = 3000\,\text{fb}^{-1}$ in the decade 2026-2036 at $\sqrt{s} = 14\,\text{TeV}$. This will be achieved by increasing the instantaneous luminosity up to $7.5 \times 10^{34}\text{cm}^{-2}\text{s}^{-1}$.

The replacement of the current Tracker with a new detector featuring higher radiation tolerance and enhanced functionality is one of the main upgrades planned for the CMS detector to maintain its excellent physics performance [1, 2]. The inner region of the new Tracker will be instrumented with an Inner Pixel detector based on hybrid pixels. A map of the expected particle fluence after $\mathcal{L}_{\text{int}} = 3000\,\text{fb}^{-1}$ in the region of the Inner Pixel is shown in figure 1. In the innermost region ($r \simeq 3\,\text{cm}$) a fluence of particles corresponding to a non-ionizing energy loss (NIEL) up to

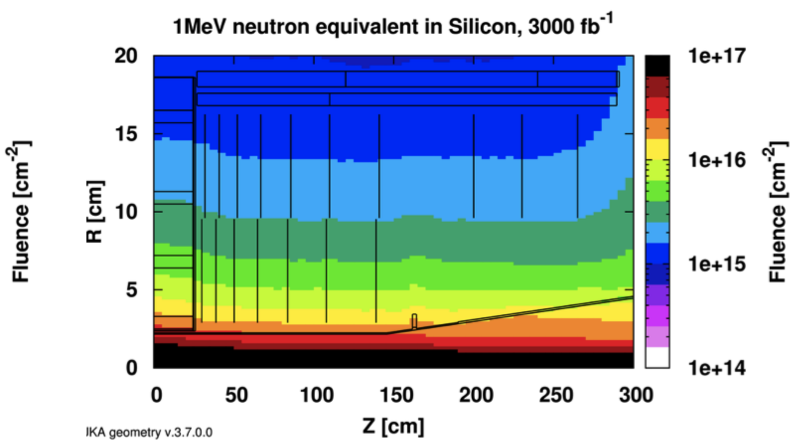

Figure 1. Map of the expected particle fluence in the CMS Inner Pixel volume corresponding to an integrated luminosity of $3000\,\text{fb}^{-1}$, expressed in terms of 1 MeV neutron equivalent fluence. The expected fluence has a strong dependence on the distance from the beamline, r-coordinate, while it is almost independent of the position along the beamline, z-coordinate [1, 2].

2016 JINST 11 C12061

$\Phi = 2 \times 10^{16}$ 1 MeV n_{eq}/cm^2 will be reached. The total ionizing dose (TID) will be about 10 MGy. The peak instantaneous luminosity with a bunch-crossing separation of 25 ns will lead to an average number of simultaneous inelastic collisions per crossing (pileup) of 200 which in the innermost region translates into a rate of charged particles of about 750 MHz/cm^2 or equivalently into a hit rate of 3 GHz/cm^2. All these values are about one order of magnitude larger than those for which the current detector was designed [3, 4]. Besides the above operational conditions, the main functional requirements driving the design of the Inner Pixel detector are:

- an extended coverage for an efficient mitigation of the pileup using techniques based on the particle-flow event reconstruction algorithm [5] which requires tracking and vertexing capabilities up to pseudorapidities η of ± 4;
- a high granularity to guarantee a low occupancy and an efficient pattern recognition especially in the dense environment of high energy jets;
- a reduced material budget, about 2.5% of a radiation length (X_0) per layer, to limit the effects of the hadronic interactions and of the multiple scattering on the reconstruction of charged particle tracks and on the measurement of their momentum.

In the following it will be discussed how these requirements are driving the design of the layout of the detector, of the sensors and of the services, respectively.

2 The layout of the Inner Pixel detector

While the layout of the Inner Pixel detector is not yet frozen, a baseline design of the system is already emerging (figure 2). This layout has been developed using a dedicated software package, tkLayout [6, 7], which estimates the resolutions on the parameters of the tracks accounting for the position of the sensing elements, the resolution on the coordinates measured at each plane and the effects of the inactive material and of the services attributed to each configuration under investigation.

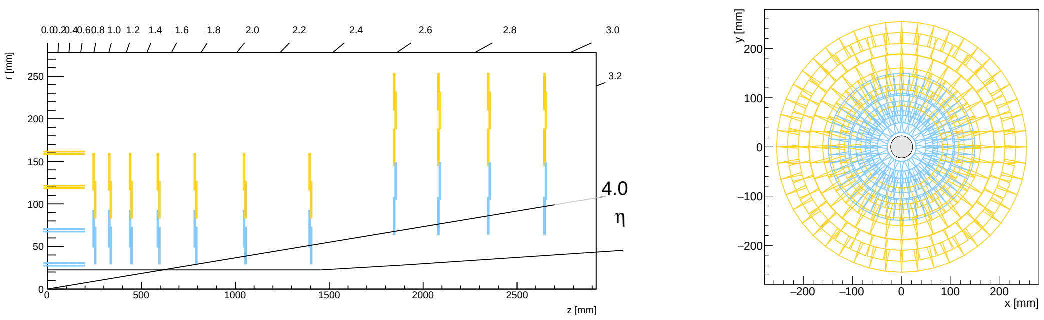

Figure 2. Layout of the CMS Inner Pixel detector. Left: sketch of one quarter (r-z view) of the detector. Right: sketch of a disc in the transverse x-y plane. Azure lines correspond to modules with small pitch pixels, yellow lines to modules with large pitch pixels.

2016 JINST 11 C12061

The Inner Pixel detector will consist of a barrel section made of four cylindrical layers extending from $r = 2.9$ cm up to $r = 16$ cm radially and up to $|z_{\mathrm{max}}| \simeq 20$ cm along the beamline. The inner envelope is dictated by the diameter of the beampipe, 6.9 cm, while the outer envelope by the presence of the Outer Tracker.[1] The arrangement of the barrel is similar, although shorter to further reduce the amount of material crossed by particles, to what is foreseen for the Phase-1 detector which will operate until the long shutdown beginning in 2023 [8]. The forward region instead will consist of 11 + 11 discs. The total instrumented surface will amount to $\sim 4.5\,\mathrm{m}^2$. To guarantee a uniform coverage in η the last four discs will start at larger radius, $r \simeq 7$ cm, and extend up to $r \simeq 30$ cm. A simple structure with discs each made of two flat "D"-shaped carbon fiber supports and tiled by rectangular or square modules is foreseen.

An additional requirement affecting the layout of the Inner Pixel detector is the possibility to install the central part of the detector with the beampipe in place. This requires additional clearance at the far edge of the detector which is achieved by introducing a step in the envelope between the Inner Pixel and the Outer Tracker, from $r \simeq 20$ cm to $r \simeq 30$ cm at $z \simeq 160$ cm.

3 The design parameters of the sensors

The baseline is to instrument the Inner Pixel with small pitch radiation tolerant planar silicon sensors with the option of using 3D sensors in the regions of the detector more exposed to irradiation. Few design parameters of the sensors have already been settled:

- *n-on-p* substrate as tests on *p-on-n* mini-strip sensors show an increase of the noise figure after $\Phi = 10^{15}\,1\,\mathrm{MeV}\;\mathrm{n_{eq}/cm^2}$ and the *n-on-n* sensors have a higher cost because of the required double-sided processing of the silicon wafer. The main challenge in using *n-on-p* sensors is to prevent sparks between the readout chip (ROC) kept at ground potential and the sensor as the high negative voltage applied to the backplane of the sensor, in absence of protection structures, extends along its edges, eventually reaching the sensor front face at few hundreds microns distance from the ROC itself. Two protection mechanisms are currently under investigation: an in-process coating of the ROC wafer and of the sensor with a benzocyclobutene (BCB) layer, easier to automate but potentially not covering the full surface as it stops at few tens of microns from the dicing line, and a post-process deposition of a Parylene layer on the full module, which requires additional manual interventions on the individual modules.[2]

- Thickness of the active area in the range 100-200 μm. This is supported by results on mini-strip sensors [9, 10] which indicate that after a NIEL typical of HL-LHC at $r \sim 4$ cm, e.g. about $10^{16}\,1\,\mathrm{MeV}\;\mathrm{n_{eq}/cm^2}$, the 100 μm thick sensors are as efficient in collecting charge as the 200 μm thick ones but operating at 200 V smaller bias voltage. On the other hand after irradiation the 100 μm thick sensors exhibit a soft-breakdown behavior beside being

[1]The inner radius of the Outer Tracker is fixed by the smallest radial separation allowed between a pair of closely spaced modules of the same layer for rejecting tracks with transverse momentum $p_T < 2\,\mathrm{GeV}/c$ in the 3.8 T magnetic field of the CMS experiment, using sensors segmented with a 100 μm pitch.

[2]Parylene coating through CVD is a process developed at Purdue's Birck Nanotechnology Center, West Lafayette, IN (United States).

2016 JINST 11 C12061

more prone to bowing and giving smaller signal ($\sim$ 7500 e) before irradiation. The optimal combination of thickness of the sensor, thickness of the active area and operating bias voltage is still to be defined.

- Pixel cells with a small pitch (2500 μm^2 area) either with a rectangular (25 $\times$ 100 μm^2) or a square (50 $\times$ 50 μm^2) aspect ratio. Technically the main challenge is the limited room for implementing the p-stop structures for insulating the individual pixels and the components for the conventional biasing scheme for testing the sensor before the assembly of the ROC. Concerning the performance, a comparison between the two geometries of the pixel cell was made using single muon Monte Carlo tracks generated and processed through the CMS detector simulation and reconstruction software. The study was repeated with two sensor thicknesses, 100 μm and 150 μm, and three thresholds for the signal in a single pixel cell (1000 e, 1500 e and 2000 e). For reference the ROC under development for the HL-LHC will feature a digital sparsified readout with a design in-time threshold around 1200 e. This study did not take into account the effects of radiation damage. The spatial resolution in the transverse plane (r-ϕ) as a function of η for the hits measured by the first layer of the barrel is shown in figure 3. Similarly the spatial resolution along the beamline (z) is shown in figure 4. In both cases the spatial resolution was derived using the known position of the particle from the Monte Carlo truth. Rectangular pixels perform better than square pixels in the transverse plane and are competitive with square pixels also in the z-coordinate. Square pixels show a deterioration of the resolution in the scenario of large thickness and high threshold. This is likely due to the breakage of the cluster occurring more frequently when a long path through the silicon is sampled many times by shorter cells. While the effect of the cluster breakage may be reduced by a better clustering algorithm, at present it is not possible to predict precisely how the signal and the noise of the single cells, and consequently the actual value of the threshold which will be applied, will be affected by the high radiation level of the HL-LHC.

  Similar studies indicate that square pixels also aggravate the bandwidth requirements with an increase of almost 30% of the hit rate at the edges of the barrel.

For investigating these issues an intense program of measurements is planned for 2017–2018 exploiting the new ROCs able to survive up to few MGy of dose and designed specifically to match the 2500 μm^2 pixels.[3] Results will be derived from batches of sensors from three different vendors: Hamamatsu, FBK and Sintef. The main features of the sensors and the goals of the three submissions are summarized in table 1.

4 The readout chain and the related services

The design of the readout chain and of the related services determines the modularity of the system and the material budget associated to it. As a reference, the overall mass of the silicon sensors for 150 μm thickness of the sensor will be about 1.6 kg.

[3] These ROCs are ROC4Sens developed by the Paul Scherrer Institut, Villigen (Switzerland), and RD53A from the RD53 Collaboration.

2016 JINST 11 C12061

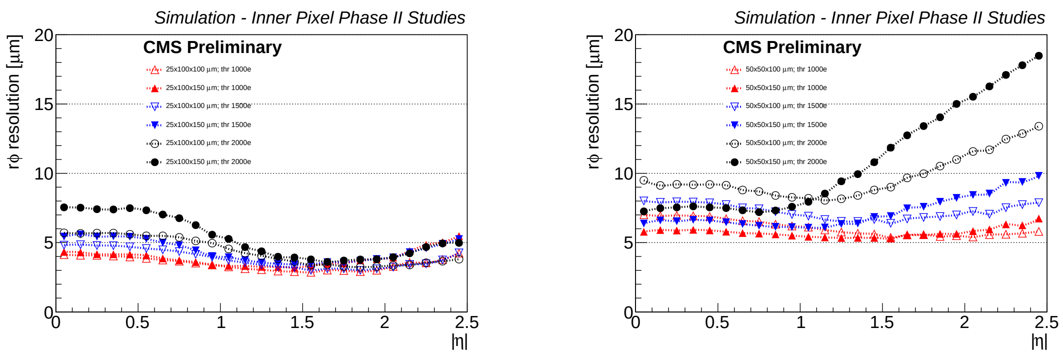

Figure 3. Hit resolution in r-ϕ as a function of η of the hit for small pitch pixels for different thresholds and sensor thicknesses (first layer of the barrel). Red: threshold = 1000 e, blue: threshold = 1500 e, black: threshold = 2000 e; open symbols: 100 μm sensor thickness, filled symbols: 150 μm sensor thickness. Left: $25 \times 100\ \mu m^2$ pixel size. Right: $50 \times 50\ \mu m^2$ pixel size. The results do not include the effects of radiation damage.

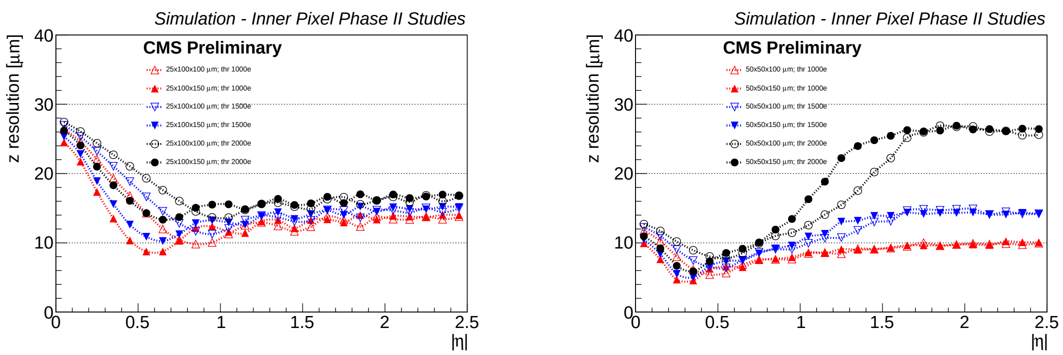

Figure 4. Hit resolution in z as a function of η of the hit for small pitch pixels for different thresholds and sensor thicknesses (first layer of the barrel). Red: threshold = 1000 e, blue: threshold = 1500 e, black: threshold = 2000 e; open symbols: 100 μm sensor thickness, filled symbols: 150 μm sensor thickness. Left: $25 \times 100\ \mu m^2$ pixel size. Right: $50 \times 50\ \mu m^2$ pixel size. The results do not include the effects of radiation damage.

Table 1. Summary of the parameters of the substrate and of the main tests planned for the three batches of planar silicon sensors that will be investigated in the R&D program for the CMS Inner Pixel detector.

Producer	Wafer characteristics	Goals of the submission
Hamamatsu Photonics	*n-on-p* active thickness: 150 μm	effect of over-metal on high bias voltage stability common p-stop vs. p-spray isolation spatial resolution of small pitch pixels (square, rectangular, “bricked” geometry)
FBK	*n-on-p* active thickness: 100–130 μm	punch-through biasing scheme spark protection using BCB different wafer thinning procedures
Sintef	*n-on-n* active thickness: 300 μm	slim edge (active area 210 μm from dicing edge) slim pixels ($25 \times 600\ \mu m^2$)

The readout chip (ROC). The ROC is one of the key elements of the entire Inner Pixel detector as it must feature:

- high radiation tolerance, up to 10 MGy of TID. This requirement is reduced to 5 MGy in case the detector can be easily replaced after few years of the HL-LHC run;
- a low noise figure, compared to the 1200 e in-time threshold, to process the small signal from small pitch pixels on thin sensors which is further reduced after the exposure to irradiation;
- a deep readout buffer and a fast readout rate to comply with the 12.5 μs latency and 750 kHz readout rate prescribed by the CMS experiment.

The baseline is to adopt a ROC designed in the 65 nm technology based on the developments of the RD53 collaboration [11, 12]. The size of the ROC will be around $2 \times 2\,\mathrm{cm}^2$.

Modularity and modules. The electrical-to-optical conversion of the readout and control signals will occur inside a low-power GBT card (LP-GBT) located at $r \sim 20$ cm and outside the barrel section as currently no optoelectronic device can tolerate the level of radiation foreseen in the innermost layer of the Inner Pixel detector. The modularity of the detector in terms of ROCs is then defined by matching the input specifications of the LP-GBT (7 input links with a bandwidth of 1.28 Gbit/s each) with the output rate of a module. The latter depends on the size of the ROC and on its geographical position. An advanced design of the module does not exist yet but likely it will be possible to build the entire Inner Pixel detector using few types of modules, e.g. made of 2×1 or 2×2 ROCs. A possible configuration for a module in the innermost layer of the barrel is shown in figure 5.

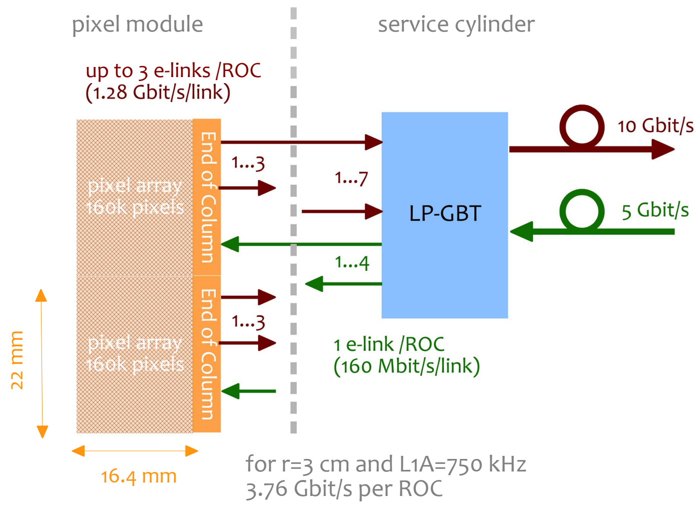

Figure 5. Possible arrangement for the readout of a module in the innermost layer of the barrel: a module made of 2×1 ROCs is readout by one LP-GBT card. In the figure one of the e-link inputs is left unconnected.

Services. The usage of a service cylinder is foreseen. The material of the services housed onto the service cylinder must be as low as possible as the service cylinder will be within the geometrical acceptance of the tracking.

The main components housed on the service cylinder will be:

- *e-link cables*: modules will be electrically connected to the LP-GBT by means of cables. A conservative estimate, which includes redundant connections, predicts a total length of the e-link cables of about 4500 m. Two options for the cables are under investigation: flex cables made of aluminum and kapton or twisted pairs based on copper conductors. Values of the total mass around 1–1.5 kg seem to be achievable. A notable point is that grounding and shielding of the cables can contribute up to 50% of the material budget of the e-link cables. Laboratory measurements of the cross-talk among cables are therefore necessary to validate the lighter configurations.

- *Power distribution*: the total power required by the Inner Pixel detector is driven by the total number of ROCs (about 12000) and by the ROC power consumption, with a maximum power consumption of about 1 W/cm^2 for a $2 \times 2\,\mathrm{cm}^2$ chip and a hit rate of 3 GHz/cm^2. An across-module serial powering scheme, where the power is supplied sequentially to clusters of chips and then distributed in parallel within each cluster, is currently under investigation as it will allow to keep the material budget of the power cables below 2 kg. With the present uncertainties, it is assumed that a total power of 40–50 kW will be required using this powering scheme.

- *Cooling system*: it will be based on a two-phase evaporative CO_2 cooling. To further reduce the material budget the usage of titanium pipes is currently under investigation.

5 Conclusions

For the HL-LHC phase, CMS will replace its pixel detector with a new Inner Pixel detector which will allow efficient tracking and vertexing under very demanding conditions and with an angular coverage extended up to $|\eta| = 4$. An intense R&D program is underway and will continue also after the publication of the Technical Design Report which is scheduled for 2017. Key points of this program will be the test of the performance of small pitch pixels before and after irradiation, the development and the test of a radiation tolerant ROC with the required functionalities in terms of latency and readout bandwidth and the setting up of a reliable system for serial power distribution.

References

[1] CMS collaboration, *Technical Proposal for the phase-II upgrade of the CMS detector*, CERN-LHCC-2015-010; LHCC-P-008; CMS-TDR-15-02 (2015).

[2] CMS collaboration, *CMS phase II upgrade Scope Document*, CERN-LHCC-2015-019; LHCC-G-165 (2015).

[3] CMS collaboration, *The CMS tracker system project: Technical Design Report*, CERN-LHCC-98-006; CMS-TDR-5 (1997).

[4] CMS collaboration, *The CMS tracker: addendum to the Technical Design Report*, CERN-LHCC-2000-016; CMS-TDR-5-add-1 (2000).

[5] CMS collaboration, *Particle-flow event reconstruction in CMS and performance for jets, taus, and MET*, CMS-PAS-PFT-09-001 (2009).

[6] S. Mersi, D. Abbaneo, N. De Maio and G. Hall, *Software package for the characterization of tracker layouts*, in *Astroparticle, particle, space physics and detectors for physics applications*, Vol. 7, World Scientific Publishing (2012), pp. 1015–1024.

[7] CMS collaboration, G. Bianchi, *tkLayout: a design tool for innovative silicon tracking detectors*, 2014 *JINST* **9** C03054.

[8] CMS collaboration, *CMS Technical Design Report for the pixel detector upgrade*, CERN-LHCC-2012-016; CMS-TDR-11 (2012).

[9] M.C. Vignali, *Silicon sensors for the upgrade of the CMS Pixel Detector*, Ph.D. thesis, Hamburg University (2015).

[10] T.V. Eichhorn, *Development of silicon detectors for the High Luminosity LHC*, Ph.D. thesis, Hamburg University (2015).

[11] J. Chistiansen, M. Garcia-Sciveres, *RD Collaboration proposal: Development of pixel readout integrated circuits for extreme rate and radiation*, CERN-LHCC-2013-008; LHCC-P-006 (2013).

[12] RD53 collaboration, *RD53A Integrated Circuit Specifications*, CERN-RD53-PUB-15-001 (2015).

2016 JINST 11 C12061